

GRAVITATIONAL WAVE SIGNAL FROM ASSEMBLING THE LIGHTEST SUPERMASSIVE BLACK HOLES

KELLY HOLLEY-BOCKELMANN¹, MIROSLAV MICIC², STEINN SIGURDSSON³, AND LOUIS J. RUBBO⁴

Draft version October 28, 2018

ABSTRACT

We calculate the gravitational wave signal from the growth of $10^7 M_{\odot}$ supermassive black holes (SMBH) from the remnants of Population III stars. The assembly of these lower mass black holes is particularly important because observing SMBHs in this mass range is one of the primary science goals for the Laser Interferometer Space Antenna (LISA), a planned NASA/ESA mission to detect gravitational waves. We use high resolution cosmological N-body simulations to track the merger history of the host dark matter halos, and model the growth of the SMBHs with a semi-analytic approach that combines dynamical friction, gas accretion, and feedback. We find that the most common source in the LISA band from our volume consists of mergers between intermediate mass black holes and SMBHs at redshifts less than 2. This type of high mass ratio merger has not been widely considered in the gravitational wave community; detection and characterization of this signal will likely require a different technique than is used for SMBH mergers or extreme mass ratio inspirals. We find that the event rate of this new LISA source depends on prescriptions for gas accretion onto the black hole as well as an accurate model of the dynamics on a galaxy scale; our best estimate yields ~ 40 sources with a signal-to-noise ratio greater than 30 occur within a volume like the Local Group during SMBH assembly – extrapolated over the volume of the universe yields ~ 500 observed events over 10 years, although the accuracy of this rate is affected by cosmic variance.

Subject headings: galaxies, intermediate mass black holes, supermassive black holes, gravitational waves, dark matter halos, n-body simulations

1. INTRODUCTION

Any mass configuration that creates a time-dependent quadrupole of the stress-energy tensor will radiate away energy in gravitational waves. One of the best examples of this is the binary pulsar system J1915+1606, whose measured orbital decay of $76 \mu\text{s}/\text{yr}$ is extremely well-described by gravitational wave emission (Hulse & Taylor 1975). However, even for very massive and compact astrophysical objects, the strain amplitude of this fluctuation in spacetime, h , is much less than 10^{-20} . For this reason, gravitational radiation has yet to be directly detected by current ground-based gravitational wave observatories such as the LIGO, VIRGO, and TAMA.

The strongest expected gravitational wave sources occur from the inspiral and merger of binary supermassive black holes. At the current epoch, nearly every galaxy is thought to host a supermassive black hole (SMBH) with a mass of $10^6 - 10^{10} M_{\odot}$ (e.g. Kormendy & Richstone 1995). Observational evidence suggests that the black holes are embedded in galactic nuclei even at high redshift, and grow more massive as the galaxy grows (e.g. Soltan 1982; David et al. 1987; Silk & Rees 1998; Kauffmann & Haehnelt 2000; Monaco et al. 2000; Schneider et al. 2002a; Granato et al. 2001; Merloni 2004). Since galaxies are thought to assemble by merg-

ing, each galaxy merger is expected to spawn a binary SMBH (Bogdanović et al. 2009; Mayer et al. 2007; Escala et al. 2006; Hopkins et al. 2005; Wyithe & Loeb 2005; Komossa et al. 2003; Menou et al. 2001; Adams et al. 2001; Haehnelt & Kauffmann 2002). In general, the inspiral and coalescence of low mass SMBHs are expected to spawn the largest amplitude gravitational wave signal (Haehnelt 1998, e.g.). The lightest SMBH binaries, with masses $10^5 - 10^7 M_{\odot}$, have coalescence frequencies between $\sim 10^{-4} - 1 \text{ Hz}$ – squarely within the frequency range of the NASA/ESA Laser Interferometer Space Antenna (LISA) which has been proposed to launch in the next decade. LISA observations will complement ground-based gravitational wave observatories by broadening the observable gravitational wave spectrum to include low frequencies. In particular, gravitational wave detections made by LISA will be able to directly map the assembly of these lightest SMBHs (Haehnelt 1994; Menou et al. 2001; Enoki et al. 2004).

In the current picture of SMBH assembly, the black hole begins life as a low mass “seed” black hole at high redshift. It’s not clear, though, when exactly these BH seeds emerge or what mass they have at birth. SMBH seeds may have been spawned from the accretion of low angular momentum gas in a dark matter halo (Koushiappas et al. 2004; Bromm & Loeb 2004), the coalescence of many seed black holes within a halo (Begelman & Rees 1978; Islam et al. 2004), or from an IMBH formed, perhaps, by runaway stellar collisions (Portegies Zwart et al. 2004; Miller & Colbert 2004; van der Marel 2004). However, the most likely candidates for SMBH seeds are the remnants that form from the first generation of stars sitting deep within dark

¹ Department of Physics and Astronomy, Vanderbilt University, Nashville, TN, 37235 Email: k.holley@vanderbilt.edu

² Center for Gravitational Wave Physics, The Pennsylvania State University, University Park, PA 16802 Email: steinn@astro.psu.edu

³ Department of Physics, University of Sydney, Sydney, Australia Email: micic@physics.usyd.edu.au

⁴ Department of Chemistry and Physics, Coastal Carolina University, Conway, SC 29528, lubbo@coastal.edu

matter halos (Madau & Rees 2001; Heger et al. 2003; Volonteri et al. 2003a; Islam et al. 2003; Wise & Abel 2005) – so called Population III stars. With masses $< 10^3 M_\odot$, these relic seeds are predicted to lie near the centers of dark matter halos between $z \sim 12 - 20$ (Bromm et al. 1999; Abel et al. 2000, 2002). Structure formation dictates that dark matter halos form in the early universe and hierarchically merge into larger bound objects, so naturally as dark matter halos merge, seed black holes sink to the center through dynamical friction and eventually coalesce. Dark matter halo mergers become synonymous, then, with black hole mergers at these masses and redshifts. This means that although the seed formation stops at $z \sim 12$ as Population III supernovae rates drop to zero (Wise & Abel 2005), SMBH growth continues as dark matter halo mergers proceed to low redshifts.

Gas accretion is thought to play a critical role in fueling the early stages of black hole growth (David et al. 1987; Kauffmann & Haehnelt 2000; Merloni 2004), and this may explain the tightness of the $M_{\text{BH}} - \sigma$ relation (Burkert & Silk 2001; Haehnelt & Kauffmann 2000; Di Matteo et al. 2005; Kazantzidis et al. 2005; Robertson et al. 2006). Since high redshift galaxies are thought to be especially gas-rich, each merger brings a fresh supply of gas to the center of the galaxy, and new fuel to the growing supermassive black hole (Mihos & Hernquist 1994; Di Matteo et al. 2003). From a combination of gas accretion and binary black hole coalescence, it is thought that these Pop III-generated seeds may form the SMBHs we observe today (Soltan 1982; Schneider et al. 2002b).

During a galaxy merger, each black hole sinks to the center of the new galaxy potential due to dynamical friction and eventually becomes bound as a binary (Kazantzidis et al. 2005; Escala et al. 2005). Dynamical friction then continues to shrink the orbit until the binary is hard (i.e. the separation between each black hole, a_{BBH} , is such that the system tends to lose energy during stellar encounters) (Heggie et al. 2007). Thereafter, further decay is mediated by 3-body scattering with the ambient stellar background until the binary becomes so close that the orbit can lose energy via gravitational radiation. In studies of static, spherical potentials, it may be difficult for stellar encounters alone to cause the binary to transition between the 3-body scattering phase and the gravitational radiation regime (Milosavljević & Merritt 2003). However, in gas-rich or non-spherical systems, the binary rapidly hardens and coalesces into one black hole, emitting copious gravitational radiation in the process (Mayer et al. 2007; Kazantzidis et al. 2005; Berczik et al. 2006; Sigurdsson 2003; Holley-Bockelmann & Sigurdsson 2006).

In our previous work, we calculated the cosmological merger rate for black holes between $200 - 3 \times 10^7 M_\odot$ from redshift 49-0 (Micic et al. 2007, 2008, (hereafter, M07)). Our approach combined high-resolution, small-volume cosmological N-body simulations with analytic prescriptions for the dynamics of merging black holes below our resolution limit; this allowed us to explore different black hole growth mechanisms and seed formation scenarios while also accurately simulating the rich and varied merger history of the host dark matter halos.

In this paper, we calculate the gravitational wave signal from the black hole mergers involved in assembling a supermassive black hole at the center of the Milky Way analogue our simulation volume. The volume is designed to provide one possible evolutionary path for a region like our Local Group, and as such, it should contain supermassive black holes on the light end of the supermassive black hole mass spectrum – the sweet spot in SMBH mass for LISA observations. We include all the mergers that have occurred from redshift 49 to the present epoch within a 1000 Mpc^3 volume of the Universe that represents a Local Group type of environment.

We found that the gravitational wave sources revealed in this volume are from much higher mass ratio mergers that the mergers predicted to be involved in assembling the most massive SMBHs. Most of the LISA science and data analysis community has been anticipating more equal mass mergers, and have developed extensive gravitational wave templates and parameter extraction techniques based on the assumption that the black hole binaries are order unity mass ratio systems (Babak et al. 2008, e.g.). While this may be true for the most massive SMBHs, we find that the black holes in our volume experience mergers with mass ratios as high as $M_2/M_1 = 10000 : 1$. These high mass ratio mergers certainly generate a different gravitational wave signal; they may even deserve a different source classification to separate it from the classical equal mass merger or extreme mass ratio inspiral⁵.

We use the rates found in our volume to extrapolate this gravitational wave signal over the Hubble Volume. Naturally, this is highly sensitive to cosmic variance, and ten runs selected from an initial larger volume are planned to mitigate cosmic variance in our merger rate estimates. However, these small volume cosmological simulations are extremely nonlinear, and as such, are computationally expensive. We are publishing the preliminary results from our first, smaller scale, simulation in order to draw the attention of the community to the interesting possibility that the assembly of the lowest mass SMBHs may involve these high mass ratio mergers and be a significant contributor to the LISA detectable event rate.

We review the details of our simulation in section 2 and in section 3, we describe how to calculate the gravitational wave signal from two merging black holes. We discuss our results and implications in section 4.

2. TRACKING THE MERGER HISTORY OF SMBHS

In Micic et al. (2008), we performed a high-resolution ‘zoom-in’ cosmological N-body simulation of a comoving section of a Λ CDM universe ($\Omega_M=0.3$, $\Omega_\Lambda=0.7$, $\sigma_8=0.9$ and $h=0.7$) from $z=49$ to $z=0$. The high resolution region was a box $10 h^{-1} \text{ Mpc}$ on each side, for a total comoving volume of $1000 h^{-3} \text{ Mpc}^3$. The volume is designed to provide one possible evolutionary path for a region like our Local Group, and as such, it should contain supermassive black holes on the light end of the supermassive black hole mass spectrum.

Our mass resolution is $8.85 \times 10^5 M_\odot$, and our spa-

⁵ Extreme mass ratio inspirals involve compact objects, like white dwarfs, neutron stars, or stellar mass black holes spiraling into a SMBH.

tial resolution is 2 kpc. After the simulation is complete, we identified halos with at least 32 particles using P-Groupfinder (Springel et al. 2001) and seed black holes those halos in the appropriate mass and redshift range to host Pop III stars. Note that we are using WMAP3 (Spergel et al. 2007) cosmological parameters in this study to compare with our previous work; however, at the time of this paper’s submission, ‘zoom-in’ simulations of several small volumes are underway with WMAP5 parameters to better explore cosmic variance. This will allow us to better pin down the rate of these new gravitational wave sources.

In our hybrid method, we combine the dark matter halo merger trees obtained in numerical simulations with an analytical treatment of the physical processes that arise in the dynamics of galaxy and black hole mergers. Since some of the processes are ill-constrained, we probe the effect of different black hole growth recipes on the final black hole mass function. In general, we assume each dark matter halo is described by an NFW profile (Navarro et al. 1997), and include the effects of dynamical friction and merger-induced gas accretion onto the SMBH, as well as the SMBH merger itself. This hybrid approach generates, for each recipe, a census of the number and mass ratio of the mergers in our volume at each redshift.

One of the surprises from this method is that the black hole mass function is quite sensitive to the dynamics of the host dark matter halo on large scales. Previous semi-analytic work on SMBH growth all assume that the host galaxies assembled from binary mergers whose timescale was dictated by Chandrasekhar dynamical friction (Chandrasekhar 1943). Numerical simulations, however, indicate that galaxies can often assemble from multiple near-simultaneous mergers, and that the merger timescale is longer than what the Chandrasekhar dynamical friction timescale suggests. Simulations indicate that the merger timescale is only smaller by a factor 3 for minor mergers at $z=0$ (Boylan-Kolchin et al. 2008), so given the myriad uncertainties in the dynamics acting in the other stages of the merger, this factor of a few was neglected. However, a longer dynamical friction timescale reduces the total number of black hole mergers in a volume of the universe by pushing some mergers to the future. For example, we found that the Boylan-Kolchin treatment for dynamical friction resulted in 1056 SMBH mergers in our volume, while Chandrasekhar dynamical friction yielded 1245 mergers. In addition, most of the current work on SMBH evolution indicates that gas accretion dominates the black hole’s growth and that this gas is funneled onto the SMBH by the merger process itself (e.g. Robertson et al. 2006; Hopkins et al. 2005; Di Matteo et al. 2003; Volonteri et al. 2003b); if the gas is driven to the center over a longer timescale, then each merger may excite a longer gas-fueled growth spurt. In the context of gravitational wave source prediction, these two effects may combine to make the SMBH mergers *louder* and at *lower frequency* than what has been predicted with a Chandrasekhar dynamical friction prediction. We will return to this in Section 4.

In this paper, we select a sample of the black hole growth recipes from Micic et al. (2008) and calculate the gravitational wave signal from each of the black hole mergers in the volume. Briefly, the recipes span two

choices for the dynamical friction timescale, and three choices for the mass ratio of the halos that excite merger-driven gas accretion onto the black hole (4:1, 10:1, and $\infty : 1$ – a.k.a. ‘dry growth’).

The next section outlines this black hole growth prescription.

2.1. SMBH Growth Prescription

The SMBH in our model grows through a combination of black hole mergers and gas accretion. To better separate the effects of gas accretion on the black hole, we include a dry growth scenario, where the black hole grows through mergers only. At high redshift, this galaxy merger-driven approach is likely a good assumption, though note that at low redshift when mergers are infrequent, secular evolution, such as bar instabilities, may dominate the gas (and therefore black hole) accretion. Integrated over the whole of a black hole lifetime, though, this major merger-driven accretion is likely to be the dominant source of gas inflow. Since the black hole growth is so strongly dependent on what fuel is driven to the center during galaxy mergers, it is important to characterize this merger-driven gas inflow, including the critical gas physics that may inhibit or strengthen this nuclear supply. We are motivated by a recent suite of numerical simulations that include radiative gas cooling, star formation, and stellar feedback to study the starburst efficiency for unequal mass ratio galaxy mergers (Cox et al. 2008), which finds that the gas inflow depends strongly on the mass ratio of the galaxy (see also, e.g. Hernquist 1989; Mihos & Hernquist 1994). This study parametrizes the efficiency of nuclear star formation (i.e. gas supply and inflow), α , as a function of galaxy mass ratio:

$$\alpha = \left(\frac{M_s}{M_p} - \alpha_0 \right)^{0.5}, \quad (1)$$

where α_0 defines the mass ratio below which there is no enhancement of nuclear star formation (i.e. gas inflow). Here, the gas accretion efficiency has a maximum of 0.56 for 1:1 halo mergers and falls to zero at α_0 . This parametrization is insensitive to the stellar feedback prescription. We use α to define how efficiently the merger funnels the galaxy’s gas to the black hole accretion disk. Our equation for α differs only slightly from the Cox et al. (2008) work in that we adjust α_0 to trigger gas inflow, while their $\alpha_0 = 0.09$.

In particular, we contrasted the black hole growth that would result from only major mergers with the growth that would occur if minor mergers were included as well. Our more conservative criterion, for example, allows black holes to accrete gas only if the mass ratio of the host dark matter halo is less than 4:1 (this is synonymous with setting $\alpha_0 = 0.25$). This cuts off the gas inflow far earlier than predicted by the galaxy merger simulations, but is useful as a conservative estimate and to compare to our previous work.

We can set an upper constraint on the final black hole mass by allowing gas accretion as long as the merging dark matter halos have a mass ratio less than 10:1 (consistent with $\alpha_0 = 0.1$). Note that $\alpha_0 = 0.09$ would imply that mass ratios less than roughly 11:1 would drive

gas inflow (Cox et al. 2008), rather than 10:1. Adopting $\alpha_0 = 0.09$ would increase the black hole mass only slightly, and since our main goal is to compare to our earlier work, we retain $\alpha_0 = 0.1$.

We used a semi-analytic formalism to calculate the dynamical friction decay time and subsequent merger timescale of each black hole once it enters a dark matter halo. Now that we have a realistic description of the merger time for each black hole within a halo, we can allow the black holes to grow for a physically-motivated accretion timescale. The accretion of gas onto both incoming and the central black hole starts when the two black holes are still widely separated, at the moment of the first pericenter passage, and continues until the black holes merge (Di Matteo et al. 2005; Colpi et al. 2007, c.f.). This sets the accretion timescale, t_{acc} , as follows: $t_{\text{acc}} = t_{\text{df}}(r=R_{\text{vir}}) - t_{\text{dyn}}(r=R_{\text{vir}})$, where $t_{\text{df}}(r=R_{\text{vir}})$ is the merger timescale including dynamical friction; and $t_{\text{dyn}}(r=R_{\text{vir}})$ is dynamical time at virial radius R_{vir} , which marks the first pericenter pass of the black hole. By stopping the accretion as the black holes merge, we roughly model the effect of black hole feedback in stopping further accretion.

Putting these pieces together, the mass accreted by a black hole during $t_{\text{acc}}(r=R_{\text{vir}})$ is:

$$M_{\text{acc}} = M_{\text{BH},0} (e^{\frac{\alpha t_{\text{acc}}}{t_{\text{sal}}}} - 1), \quad (2)$$

where $M_{\text{BH},0}$ is initial black hole mass, and α is starburst efficiency (Cox et al. 2008), and $t_{\text{sal}} \equiv \epsilon M_{\text{BH},0} c^2 / [(1 - \epsilon)L]$, where ϵ is the radiative efficiency, L is the luminosity, and c is the speed of light. After t_{df} , the incoming black hole merges with the SMBH at the center and a new SMBH is formed after having accreted gas for t_{acc} . The accretion time and efficiency both implicitly encode the large-scale dynamics of the merger and the bulk gas accretion into the nuclear region, while t_{sal} describes the accretion disk physics. As before, we set t_{sal} to describe sustained Eddington-limited accretion with a efficiency of $\epsilon = 0.1$ (Shakura & Sunyaev 1973).

In Micic et al. (2008), we found that a gas accretion triggered by major mergers (4:1) and a Boylan-Kolchin dynamical friction prescription produced a $4 \times 10^6 M_{\odot}$ SMBH from a $200 M_{\odot}$ seed in place by $z=5$. We consider this our preferred model as it produces a SMBH consistent with the Sgr A*. Note, however, that the minor merger (10:1) Boylan-Kolchin prescription also generates a $1.3 \times 10^7 M_{\odot}$ black hole from the same seed, and can be considered a viable model for an M31-like SMBH.

3. CALCULATING THE GRAVITATIONAL WAVE SIGNAL

In order to compare our results with other published results, we follow the approach of Sesana et al. (2004) to calculate the gravitational wave signal from the black hole mergers in our simulation volume. In this section, we provide a brief background on the theory and outline the method; for a more in-depth description of gravitational waves from SMBHs see, for example, Berti (2006).

The orbital motion of the binary system constitutes will excite a time-dependent mass quadrupole, which generates gravitational radiation. The gravitational wave strain, h , measures the strength of the propagating wave. The amplitude depends on the comoving distance

to the binary, d , the rest frame gravitational wave frequency, f_r , and the chirp mass of the binary, \mathcal{M} . The rest-frame gravitational wave frequency is related to the orbital period, P , of the binary, $f_r = 2/P$, and the chirp mass depends on the mass of each binary component as follows: $\mathcal{M} \equiv (m_1 m_2)^{3/5} / (m_1 + m_2)^{1/5}$. When averaged over the sky position, polarization, and period, the strain can be written as:

$$h = \frac{8\pi^{2/3} G^{5/3} \mathcal{M}^{5/3}}{10^{1/2} c^4 d} f_r^{2/3}. \quad (3)$$

This gravitational radiation will cause the binary components to inspiral on ever tighter and faster orbits. When massive black hole binaries are widely separated and orbiting at low frequencies, the gravitational radiation emitted is relatively weak, and therefore the frequency shift per orbit is minuscule. Most of the evolution is spent in this phase, where a frequency shift of order unity takes many orbits to achieve.

As the binary separation slowly shrinks, the gravitational radiation emitted increases dramatically until the binary coalesces. Close to coalescence, the binary rapidly sweeps through many frequencies in one orbit, and at the innermost stable circular orbit (ISCO), the change in frequency per orbit is of order unity.

We set the minimum observed frequency to f_{ISCO} for a test particle orbiting around a single Schwarzschild black hole. In the black hole mergers we consider, the mass ratios are always well outside this test particle limit; we adopt the conventional definition for f_{ISCO} nonetheless:

$$f_{\text{ISCO}} = \frac{c^3}{6^{3/2} \pi G} \frac{1}{(m_1 + m_2)} (1+z)^{-1}, \quad (4)$$

where c and G are the speed of light and gravitational constant, respectively, m_1 and m_2 are the black hole masses, and z is the redshift.

The frequency shift rate in the rest-frame is, to first order:

$$\dot{f}_r = \frac{96\pi^{8/3} G^{5/3}}{5c^5} f_r^{11/3} \mathcal{M}^{5/3}. \quad (5)$$

The orbital periods of million solar mass black hole binaries in the gravitational radiation regime are on the order of hours, which means that multi-year observations could accumulate many cycles of an inspiral at a particular frequency. LISA, for example, is expected to observe the sky for at least a year, and projections place the LISA lifespan at roughly a decade. Million solar mass black holes orbiting in the LISA frequency band of $\sim 10^{-4} - 1$ Hz are years or less from coalescence, so LISA observations will be able to track the inspiral and coalescence phases of supermassive black hole binaries. The number of cycles accumulated during the inspiral in an observation of duration τ depends on the observed gravitational wave frequency, $n = f\tau$, where $f = f_r/(1+z)$. Note that there are two regimes: $f > n/\tau$, where the binary sweeps through many frequencies in an observation, and $f < n/\tau$, where the signal builds from several orbits at one frequency.

The observed characteristic strain, h_c , is the strain accumulated a single observation:

$$h_c = h\sqrt{n} \sim \frac{1}{\sqrt{3}\pi^{2/3}} \frac{G^{5/6} \mathcal{M}^{5/6}}{c^{3/2} d} f_r^{-1/6} \quad n < f\tau, \quad (6)$$

$$h_c = h\sqrt{f\tau} \sim \frac{8\pi^{2/3} G^{5/3} \mathcal{M}^{5/3}}{10^{1/2} c^4 d} f_r^{7/6} \tau \quad n > f\tau. \quad (7)$$

Since we have the component mass and redshift of each black hole merger in our simulation volume, we can calculate h and h_c over an observation span τ before merger. Most black holes in our volume will merge within a year of reaching the LISA band, so a 3-year observation window should catch these mergers in the act – if this volume is a representative slice of the Universe. We distinguish between the mergers directly found in our volume and the mergers extrapolated throughout the Universe in Table 2.

4. RESULTS

4.1. A New Gravitational Wave Source

Overall, most of the mergers in our volume are between seed and intermediate mass black holes ($O(10^4) M_\odot$) at redshifts greater than 5 (Figure 1). Though these mergers were critical in assembling the eventual SMBH in our Milky Way analogue, the generated LISA signal-to-noise ratio of most of these low mass mergers at high redshift were much less than 1.0. Figure 7 demonstrates that the overwhelming majority of black hole mergers will fall below LISA’s detection limit. Although there are a few mergers that are resolvable by LISA at $z > 6$, the number of resolvable sources increases once the SMBH grows to a mass within the LISA band at $z < 5$, as can be seen in Figure 8. This broadly agrees with Sesana et al. (2005), which showed that $\sim 10\%$ of the precursors to $10^9 M_\odot$ SMBHs are expected to be observable with LISA out to redshift 10.

However, Figure 1 also reveals a substantial class of black hole mergers with very high mass ratios; these arise from the accretion of smaller satellite halos at low redshift. Since these mergers are nearby, they are easily detectable with LISA. This is in stark contrast to the predictions for assembling the massive end of the SMBH mass spectrum; Sesana et al. (2007) showed that the detectable mass ratios are equally distributed in the range of 1-10. In fact, Figure 4 indicates that the most commonly observed black hole mergers in our volume have mass ratios of 1000 or more (depending on the black hole growth prescription). Mergers of more equal mass dark matter halos (and subsequently, the coalescence of more equal mass black holes) occurred in this volume at $z > 8$, and at this epoch, most of our black holes were too small to be observed by LISA. Figures 1 and 3 bear this out by plotting mapping the number of resolvable sources as a function of mass ratio and redshift for one black hole growth prescription over a 10 year observation.

The signals from an equal mass inspiraling system and those with mass ratios of upwards of ten thousand can be quite different. From an analytical standpoint, the difference in signals can be understood by investigating the post-Newtonian expansion of the gravitational wave strain, which uses the orbital velocity as an expansion parameter. Each term in the expansion results in harmonics of the orbital frequency Blanchet et al. (1996). Starting at the first full order, certain select frequencies are scaled by $\eta \equiv m_1 m_2 / (m_1 + m_2)^2$, which suppresses those frequencies for systems with large mass ratios. Figure 6 compares the power spectral densities for two SMBH systems: one with two $10^7 M_\odot$ SMBHs and

the other with $m_1 = 10^7 M_\odot$ and $m_2 = 10^4 M_\odot$. These figures demonstrate how the equal mass system sweeps through all frequencies while the large mass ratio system shows much more structure, with many of the frequencies being suppressed.

The LISA data streams present unique challenges for data mining. Unlike electromagnetic observatories, LISA is simultaneously sensitive to gravitational wave sources located all throughout the sky. LISA will also be sensitive to a wide variety of astrophysical sources – from supermassive black hole binaries, to millions of close white dwarf binaries within our galaxy, to EMRIs. The data analysis objective is to conclusively detect a signal and to extract descriptive parameter values. In preparation for the immense data analysis challenge, simulated data has been produced and distributed to the LISA community as part of the Mock LISA Data Challenge (MLDC) Vallisneri (2009). So far the challenges have focused on order unity mass ratios for the simulated supermassive black hole inspirals. While for most analysis techniques an assumption about the mass ratio is not hardwired into the routine, the routines have not been tested at the more extreme ratios of 10^5 as suggested here. It is possible that the suppressed harmonics will cause false-positives or negatives in some routines because the system will be missed or misidentified.

4.2. The LISA Signal from Assembling a Milky Way SMBH

Figure 9 presents the total characteristic strain for 7 bright black hole mergers in our volume, assuming a 10:1 black hole growth recipe and a Boylan-Kolchin dynamical friction treatment. The differences in the two classes of source is clear – the brightest sources are high mass ratio mergers which coalesce in the LISA band at low redshift, while the other bright class probes more equal-mass mergers of low mass black holes at high redshift. Note that the black holes in the bottom-most track actually merge outside the LISA band and will be considered an inspiral; this was the only detectable inspiral in our volume.

In Table 1, we determined the redshift at which these 7 mergers would become undetectable in a 3 year observation. Understandably, the highly unequal mass mergers can only be detected out to a luminosity distance of roughly 3 Gpc, which is similar to the distance probed by extreme mass ratio inspirals (Gair et al. 2004). LISA observations of this class of high mass ratio merger, then, may be useful to probe the fraction of black hole mass is accreted at late times for this low mass SMBH range.

Figure 5 presents the total characteristic strain for the LISA detector from all the black hole mergers in our $1000 \text{ h}^{-3} \text{ Mpc}^3$ volume over a 3-year observation span. Each curve has a low frequency rise that drops steeply off before hitting a shallow plateau; the rise and drop-off is the signature of the accumulated high mass ratio mergers, while the shallow segment marks the sum of the relatively equal mass mergers. We caution that this implicitly assumes that all of these mergers would take place during this 3-year period, or alternatively that this volume is representative of the Universe. Issues of cosmic variance aside, we can see that the black hole growth prescription strongly influences the total strain in the LISA band; this is best seen when dynamical friction

is described by Boylan-Kolchin et al. (2008) where the drop-off changes by a decade in frequency in response to a change in the typical mass of the local SMBHs.

4.3. *Extrapolating to Universal Black Hole Merger Rates*

Although this is plagued by cosmic variance, it is instructive to estimate the number of mergers observable by LISA in the Universe expected from assembling these lightest SMBHs. Table 2 presents the extrapolated Universal LISA merger rates. One surprising point is that the LISA merger rates depend so strongly on the adopted form of the dynamical friction force. All previous LISA merger rate estimates have used a semi-analytic technique that employs Chandrasekhar dynamical friction to merge the dark matter halos and to usher the black holes to the inner kiloparsec. However, both perturbation theory (Colpi et al. 1999) and numerical simulations (Weinberg 1989; Holley-Bockelmann & Richstone 1999; Boylan-Kolchin et al. 2008) have shown that Chandrasekhar dynamical friction approximates the merger time to within a factor of two, at best. When we employ a dynamical friction formalism that is based on fits to merger timescales from numerical simulations, we find that the black hole mergers are delayed to lower redshift. Naively, this would simply make every merger louder. However, in our SMBH growth prescription, there is an additional effect: since the incoming SMBH drives gas inflow to the primary SMBH over a longer timespan, resulting SMBH ultimately grows more massive than with Chandrasekhar dynamical friction. This can place the SMBHs in our volume just out of LISA’s ‘sweet spot’ which will decrease the signal-to-noise ratio of the more massive black holes. Paradoxically, then, the LISA event rate for more correct merger times drops by as much as an order of magnitude. For our most realistic model to assemble the lightest SMBHs – gas accretion triggered by major mergers, with a Boylan-Kolchin dynamical friction merger timescale – the merger rate drops by a factor of two. Over a 3 year LISA observation, we should be able to detect at least 70 SMBH mergers with a signal-to-noise ratio greater than 30 that are involved in assembling the light end of the SMBH mass spectrum in the Universe. If we consider longer LISA observation windows, the number of observed sources increases, naturally, and for a 10 year observation, LISA should detect nearly 500 mergers from the assembly of the lightest SMBHs alone.

5. DISCUSSION

By concentrating on a small cosmological volume, we have been able to model the gravitational wave sources that result from the assembly of a $\sim 10^6 - 10^7 M_\odot$ black hole in a Milky Way mass halo. We have calculated the gravitational wave strain for each of the black hole mergers in our volume, and have determined which of those will be detectable with LISA. Of the 1500 mergers in our volume, we uncovered approximately 300 – 1200 mergers detectable with a signal-to-noise ratio greater than 5 over a LISA observation span of 3 years.

We found that the most common class of observable black hole merger in our volume is between a SMBH and IMBH (of 200-2000 M_\odot) at $z < 0.05$. These IMBHs originally resided in small dark matter halos that merged with the massive primary halo at high redshift and had very

long dynamical friction timescales. Before the merger occurs, the incoming IMBH may be observed with the next generation of X-ray telescopes as a ULX source with a rate of about $\sim 3 - 7 \text{ yr}^{-1}$ for $1 \leq z \leq 5$. Because of their potential tie to observable ULXs, and because this class of source has a different waveform character than other well known gravitational wave sources, such as equal mass mergers, intermediate mass ratio inspirals (IMRIs), or extreme mass ratio inspirals (EMRIs), we have nominally dubbed this class of source as an Ultra Large Inspirals (ULIs). The other class was IMBH-IMBH mergers at $z = 2 - 8$.

Note that we could not resolve the growth of the most massive dark matter halos with our technique, and miss the mergers that arise from the assembly of the most massive SMBHs. Therefore, we consider our approach to be complementary to studies like Sesana et al. (2005, 2007) – we believe that the high mass ratio mergers identified here would add to the rates found in previous studies that focus on black hole growth in present-day halos larger than $\sim 10^{11} M_\odot$. However, the high mass-ratio channel that we have identified may well dominate the LISA black hole merger events. In fact, even our most pessimistic estimate (~ 70 events) yields a comparable number of LISA sources as Sesana et al. (2005) (~ 90 events).

The signal-to-noise ratio listed in Table 1 assumes simple data analysis techniques. If we were to employ similar sophisticated tools as are being developed for the extreme mass ratio inspirals, such as matched filtering, it is possible that this class of source may probe slightly larger distances than EMRIs. In any event, current data analysis techniques to extract SMBH signals from LISA data streams all assume the binaries have mass ratios close to unity. As we have shown here, the more complex waveform structure of these ULIs may require a different data analysis strategy.

In our volume, the SMBH was in place at nearly its final mass at redshift 5, and it was built by mergers of hundreds of $O(10^2) M_\odot$ black holes at $z > 5$ – these mergers were too weak to be detectable by LISA. In fact, the first trace of the growing SMBH occurs at about redshift 7 for our most aggressive gas accretion prescription. This may have implications for how well LISA observations can constrain the early growth of these lightest SMBHs.

In this paper, we have neglected gravitational wave recoil, a potentially important mechanism that may inhibit black hole growth. Binary black holes strongly radiate linear momentum in the form of gravitational waves during the plunge phase of the inspiral – resulting in a “kick” to the new black hole. This, in itself, has long been predicted as a consequence of an asymmetry in the binary orbit or spin configuration. Previous kick velocity estimates, though, were either highly uncertain or suggested that the resulting gravitational wave recoil velocity was relatively small, astrophysically speaking. Now, recent results indicate the recoil can drive a gravitational wave kick velocity as fast as $\sim 4000 \text{ km s}^{-1}$ (e.g. Herrmann et al. 2007; Gonzalez et al. 2006; González et al. 2007; Baker et al. 2006; Koppitz et al. 2007; Campanelli et al. 2007; Schnittman & Buonanno 2007). In reality, much smaller values than this maximum may be expected in gas-rich galaxies due to the alignment of the orbital angular momentum and spins

of both black holes (Bogdanović et al. 2007). However, even typical kick velocities ($\sim 200 \text{ km s}^{-1}$) are interestingly large when compared to the escape velocity of typical astronomical systems – low mass galaxies, as an example, have an escape velocity of $\sim 200 \text{ km s}^{-1}$ (e.g. Holley-Bockelmann et al. 2008). The effect of large kicks combined with low escape velocity from the centers of small dark matter halos at high redshift plays a major role in suppressing the growth of black hole seeds into SMBH. Even the most massive dark matter halo at $z \geq 11$ can not retain a black hole that receives $\geq 150 \text{ km s}^{-1}$

kick (Merritt et al. 2004; Micic et al. 2006). We have submitted a companion paper that incorporates the effect of recoil velocity on the expected merger rates and the growth of a Milky Way-mass SMBH, and find that if there is no spin alignment mechanism, then a Pop III seed black hole can reach $10^6 M_{\odot}$ only 20% of the time through merger-driven gas accretion. We are exploring the effect of recoil on the gravitational wave signal in a forthcoming paper.

ACKNOWLEDGMENTS

REFERENCES

- Abel, T., Bryan, G. L., & Norman, M. L. 2000, *ApJ*, 540, 39
—, 2002, *Science*, 295, 93
Adams, F. C., Graff, D. S., & Richstone, D. O. 2001, *ApJ*, 551, L31
Babak, S. et al. 2008, *Classical and Quantum Gravity*, 25, 184026, proceedings of the 12th Gravitational Wave Data Analysis Workshop
Baker, J. G., Centrella, J., Choi, D.-I., Koppitz, M., van Meter, J. R., & Miller, M. C. 2006, *ApJ*, L93
Begelman, M. C. & Rees, M. J. 1978, *MNRAS*, 185, 847
Berczik, P., Merritt, D., Spurzem, R., & Bischof, H.-P. 2006, *ApJ*, 642, L21
Berti, E. 2006, *Classical and Quantum Gravity*, 23, S785, proceedings of the 10th Gravitational Wave Data Analysis Workshop
Blanchet, L., Iyer, B. R., Will, C. M., & Wiseman, A. G. 1996, *Classical and Quantum Gravity*, 13, 575
Bogdanović, T., Eracleous, M., & Sigurdsson, S. 2009, *ApJ*, 697, 288
Bogdanović, T., Reynolds, C. S., & Miller, M. C. 2007, *ApJ*, 661, L147
Boylan-Kolchin, M., Ma, C.-P., & Quataert, E. 2008, *MNRAS*, 383, 93
Bromm, V., Coppi, P. S., & Larson, R. B. 1999, *ApJ*, 527, L5
Bromm, V. & Loeb, A. 2004, *New Astronomy*, 9, 353
Burkert, A. & Silk, J. 2001, *ApJ*, 554, L151
Campanelli, M., Lousto, C. O., Zlochower, Y., & Merritt, D. 2007, *Phys. rev. Lett.*, 98, 231102
Chandrasekhar, S. 1943, *ApJ*, 97, 255
Colpi, M., Dotti, M., Mayer, L., & Kazantzidis, S. 2007, *ArXiv e-prints*
Colpi, M., Mayer, L., & Governato, F. 1999, *ApJ*, 525, 720
Cox, T. J., Jonsson, P., Somerville, R. S., Primack, J. R., & Dekel, A. 2008, *MNRAS*, 384, 386
David, L. P., Durisen, R. H., & Cohn, H. N. 1987, *ApJ*, 313, 556
Di Matteo, T., Croft, R. A. C., Springel, V., & Hernquist, L. 2003, *ApJ*, 593, 56
Di Matteo, T., Springel, V., & Hernquist, L. 2005, *Nature*, 433, 604
Enoki, M., Inoue, K. T., Nagashima, M., & Sugiyama, N. 2004, *ApJ*, 615, 19
Escala, A., Larson, R. B., Coppi, P. S., & Mardones, D. 2005, *ApJ*, 630, 152
Escala, A., Larson, R. B., Coppi, P. S., & Mardones, D. 2006, in *Revista Mexicana de Astronomia y Astrofisica*, vol. 27, Vol. 26, *Revista Mexicana de Astronomia y Astrofisica Conference Series*, 141–142
Gair, J. R., Barack, L., Creighton, T., Cutler, C., Larson, S. L., Phinney, E. S., & Vallisneri, M. 2004, *Classical and Quantum Gravity*, 21, 1595
González, J. A., Hannam, M., Sperhake, U., Brüggmann, B., & Husa, S. 2007, *Physical Review Letters*, 98, 231101
Gonzalez, J. A., Sperhake, U., Brüggmann, B., Hannam, M., & Husa, S. 2006, preprint (gr-qc/0610154)
Granato, G. L., Silva, L., Monaco, P., Panuzzo, P., Salucci, P., De Zotti, G., & Danese, L. 2001, *MNRAS*, 324, 757
Haehnelt, M. G. 1994, *MNRAS*, 269, 199
Haehnelt, M. G. 1998, in *Laser Interferometer Space Antenna: Second International LISA Symposium on the Detection and Observation of Gravitational Waves in Space*, ed. W. M. Folkner, Vol. 456 (Woodbury: AIP Conference Proceedings), 45–49
Haehnelt, M. G. & Kauffmann, G. 2000, *MNRAS*, 318, L35
—, 2002, *MNRAS*, 336, L61
Heger, A., Fryer, C. L., Woosley, S. E., Langer, N., & Hartmann, D. H. 2003, *ApJ*, 591, 288
Heggie, D. C., Hut, P., Mineshige, S., Makino, J., & Baumgardt, H. 2007, *PASJ*, 59, L11
Hernquist, L. 1989, *Nature*, 340, 687
Herrmann, F., Hinder, I., Shoemaker, D., Laguna, P., & Matzner, R. A. 2007, gr-qc/0701143
Holley-Bockelmann, K., Gültekin, K., Shoemaker, D., & Yunes, N. 2008, *ApJ*, 686, 829
Holley-Bockelmann, K. & Richstone, D. 1999, *ApJ*, 517, 92
Holley-Bockelmann, K. & Sigurdsson, S. 2006, *ArXiv Astrophysics e-prints*
Hopkins, P. F., Hernquist, L., Cox, T. J., Di Matteo, T., Martini, P., Robertson, B., & Springel, V. 2005, *ApJ*, 630, 705
Hulse, R. A. & Taylor, J. H. 1975, *ApJ*, 195, L51
Islam, R. R., Taylor, J. E., & Silk, J. 2003, *MNRAS*, 340, 647
—, 2004, *MNRAS*, 354, 427
Kauffmann, G. & Haehnelt, M. 2000, *MNRAS*, 311, 576
Kazantzidis, S., Mayer, L., Colpi, M., Madau, P., Debattista, V. P., Wadsley, J., Stadel, J., Quinn, T., & Moore, B. 2005, *ApJ*, 623, L67
Komossa, S. et al. 2003, *Astrophys. J.*, 582, L15
Koppitz, M., Pollney, D., Reisswig, C., Rezzolla, L., Thornburg, J., Diener, P., & Schnetter, E. 2007, *ArXiv General Relativity and Quantum Cosmology e-prints*
Kormendy, J. & Richstone, D. 1995, *ARA&A*, 33, 581
Koushiappas, S. M., Bullock, J. S., & Dekel, A. 2004, *MNRAS*, 354, 292
Madau, P. & Rees, M. J. 2001, *ApJ*, 551, L27
Mayer, L., Kazantzidis, S., Madau, P., Colpi, M., Quinn, T., & Wadsley, J. 2007, *Science*, 316, 1874
Menou, K., Haiman, Z., & Narayanan, V. K. 2001, *ApJ*, 558, 535
Merloni, A. 2004, *MNRAS*, 353, 1035
Merritt, D., Milosavljevic, M., Favata, M., Hughes, S. A., & Holz, D. E. 2004, *Astrophys. J.*, 607, L9
Micic, M., Abel, T., & Sigurdsson, S. 2006, *MNRAS*, 372, 1540
Micic, M., Holley-Bockelmann, K., & Sigurdsson, S. 2008, *ArXiv e-prints*, 805
Micic, M., Holley-Bockelmann, K., Sigurdsson, S., & Abel, T. 2007, *MNRAS*, 380, 1533
Mihos, J. C. & Hernquist, L. 1994, *ApJ*, 425, L13
Miller, M. C. & Colbert, E. J. M. 2004, *International Journal of Modern Physics D*, 13, 1
Milosavljevic, M. & Merritt, D. 2003, *ApJ*, 596, 860
Monaco, P., Salucci, P., & Danese, L. 2000, *MNRAS*, 311, 279
Navarro, J. F., Frenk, C. S., & White, S. D. M. 1997, *ApJ*, 490, 493
Portegies Zwart, S. F., Baumgardt, H., Hut, P., Makino, J., & McMillan, S. L. W. 2004, *Nature*, 428, 724
Robertson, B., Hernquist, L., Cox, T. J., Di Matteo, T., Hopkins, P. F., Martini, P., & Springel, V. 2006, *ApJ*, 641, 90
Schneider, R., Ferrara, A., Natarajan, P., & Omukai, K. 2002a, *ApJ*, 571, 30

- . 2002b, *ApJ*, 571, 30
- Schnittman, J. D. & Buonanno, A. 2007, *ApJ*, 662, L63
- Sesana, A., Haardt, F., Madau, P., & Volonteri, M. 2004, *ApJ*, 611, 623
- . 2005, *ApJ*, 623, 23
- Sesana, A., Volonteri, M., & Haardt, F. 2007, *MNRAS*, 377, 1711
- Shakura, N. I. & Sunyaev, R. A. 1973, *A&A*, 24, 337
- Sigurdsson, S. 2003, *Classical and Quantum Gravity*, 20, 45
- Silk, J. & Rees, M. J. 1998, *A&A*, 331, L1
- Soltan, A. 1982, *MNRAS*, 200, 115
- Spiegel, D. N., Bean, R., Doré, O., Nolta, M. R., Bennett, C. L., Dunkley, J., Hinshaw, G., Jarosik, N., Komatsu, E., Page, L., Peiris, H. V., Verde, L., Halpern, M., Hill, R. S., Kogut, A., Limon, M., Meyer, S. S., Odegard, N., Tucker, G. S., Weiland, J. L., Wollack, E., & Wright, E. L. 2007, *ApJS*, 170, 377
- Springel, V., White, S. D. M., Tormen, G., & Kauffmann, G. 2001, *MNRAS*, 328, 726
- Vallisneri, M. 2009, *Classical and Quantum Gravity*, 26, 094024, proceedings of the 7th International LISA Symposium
- van der Marel, R. P. 2004, in *Coevolution of Black Holes and Galaxies*, ed. L. C. Ho, 37–+
- Volonteri, M., Haardt, F., & Madau, P. 2003a, *ApJ*, 582, 559
- . 2003b, *ApJ*, 582, 559
- Weinberg, M. D. 1989, *MNRAS*, 239, 549
- Wise, J. H. & Abel, T. 2005, *ApJ*, 629, 615
- Wyithe, J. S. B. & Loeb, A. 2005, *ApJ*, 634, 910

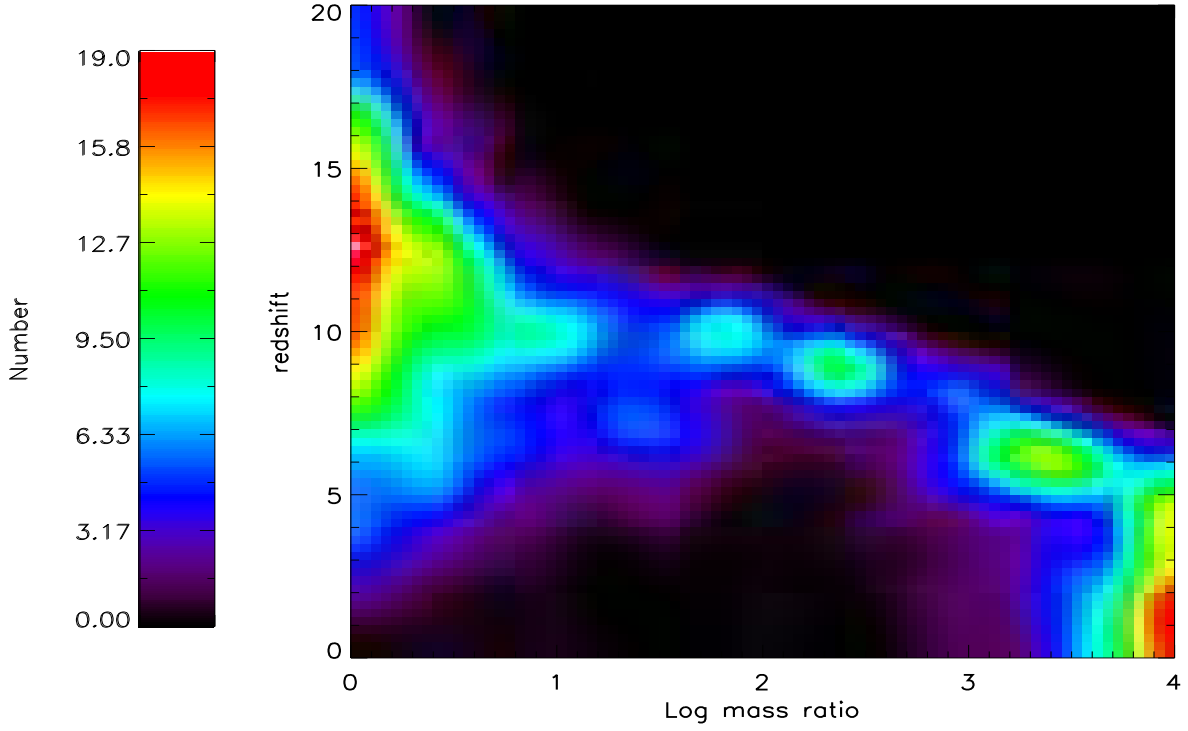


FIG. 1.— Map of the number of black hole mergers in our 1000 Mpc^3 volume as a function of the log of the black hole mass ratio and the redshift of coalescence. The colors represent the number of black hole mergers, with a scaling as denoted by the colorbar to the left of the map. Here, the dynamical friction is treated with a Boylan-Kolchin formula and gas accretion is triggered for dark matter halo mass mergers with mass ratios smaller than 4:1 – major mergers. Note the bimodal distribution, and the fact that most mergers are low mass and large mass ratio.

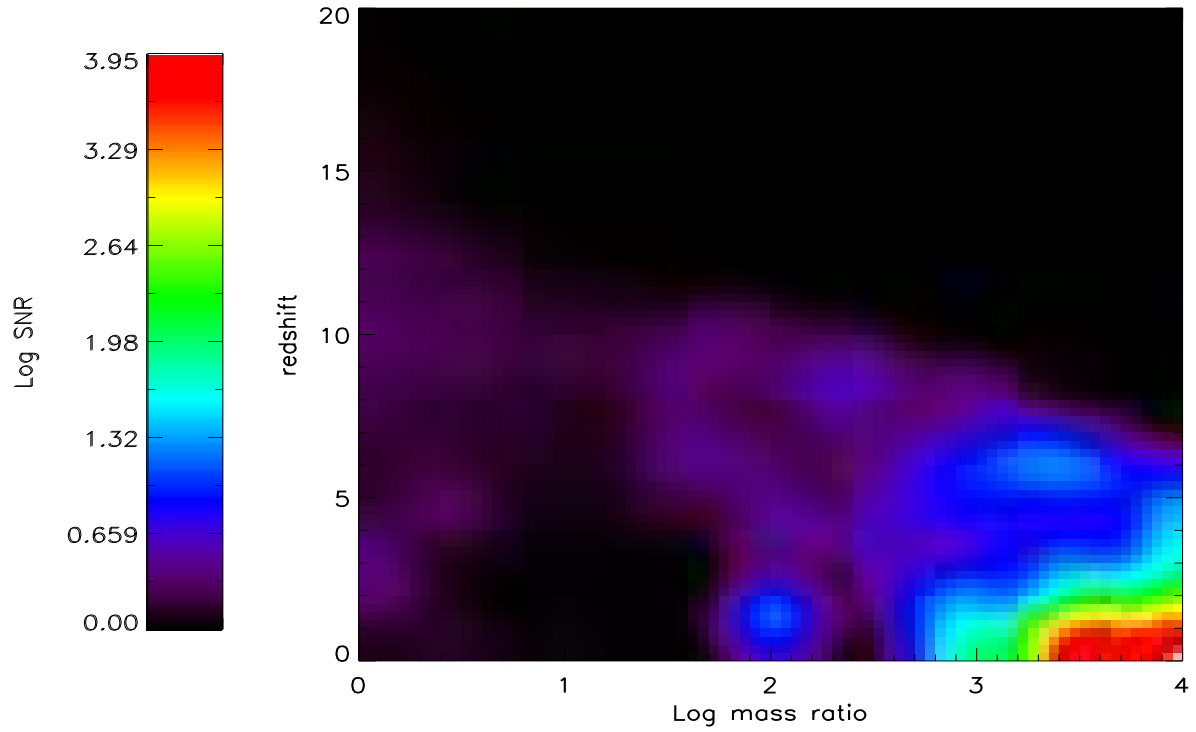


FIG. 2.— Map of the log of the signal-to-noise ratio as a function of the log of the black hole mass ratio and the redshift of coalescence. The colorbar to the left translates the colorscale to the log of the SNR – an SNR of 5 would be dark blue. Here, the dynamical friction is treated with a Boylan-Kolchin formula and gas accretion is triggered for dark matter halo mergers with mass ratios smaller than 4:1 – major mergers. Over this 10 year LISA observation, we can expect to detect no equal mass mergers, but that the loud sources will all have mass ratios larger than 100. We reemphasize that this map tracks the sources only from the formation channel of the lightest SMBHs.

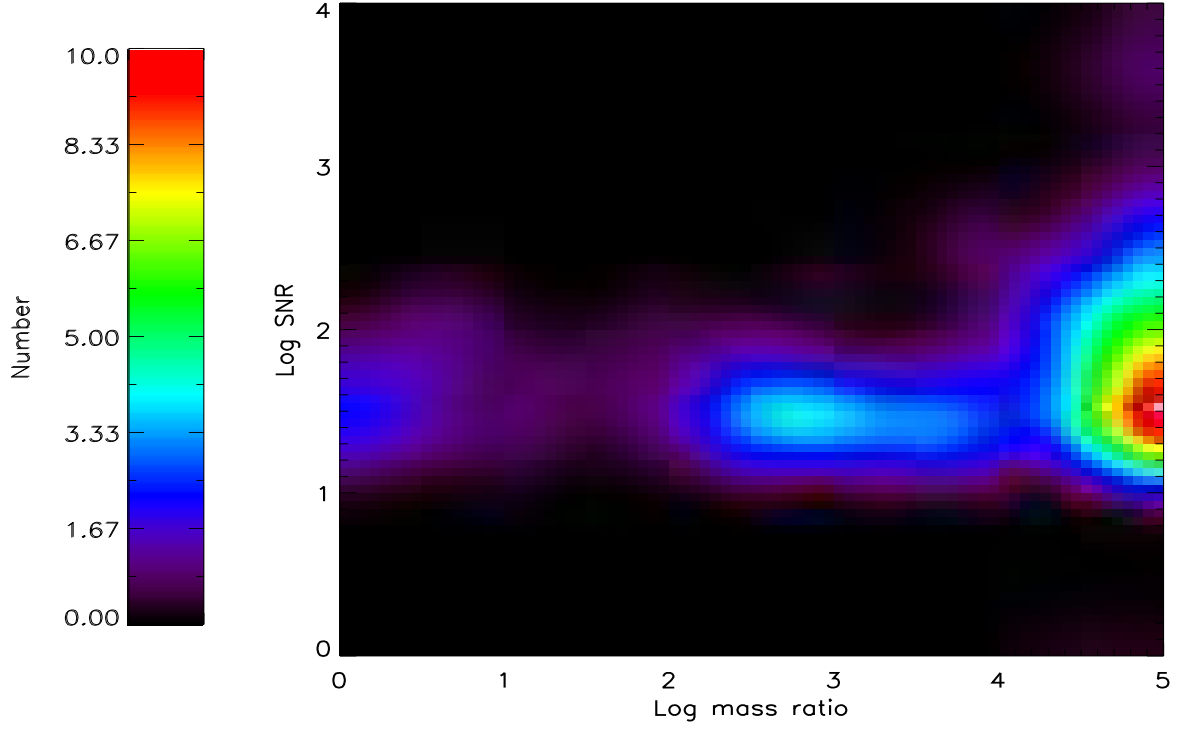


FIG. 3.— Map of the number of *resolvable* sources as a function of the log of the black hole mass ratio and the redshift of coalescence. The colorbar to the left translates the color to the number of resolvable sources with a signal-to-noise ratio is greater than 5. Here, the dynamical friction is treated with a Boylan-Kolchin formula and gas accretion is triggered for dark matter halo mergers with mass ratios smaller than 10:1 – minor mergers. Over a 10 year LISA observation, this model is dominated by high mass ratio mergers.

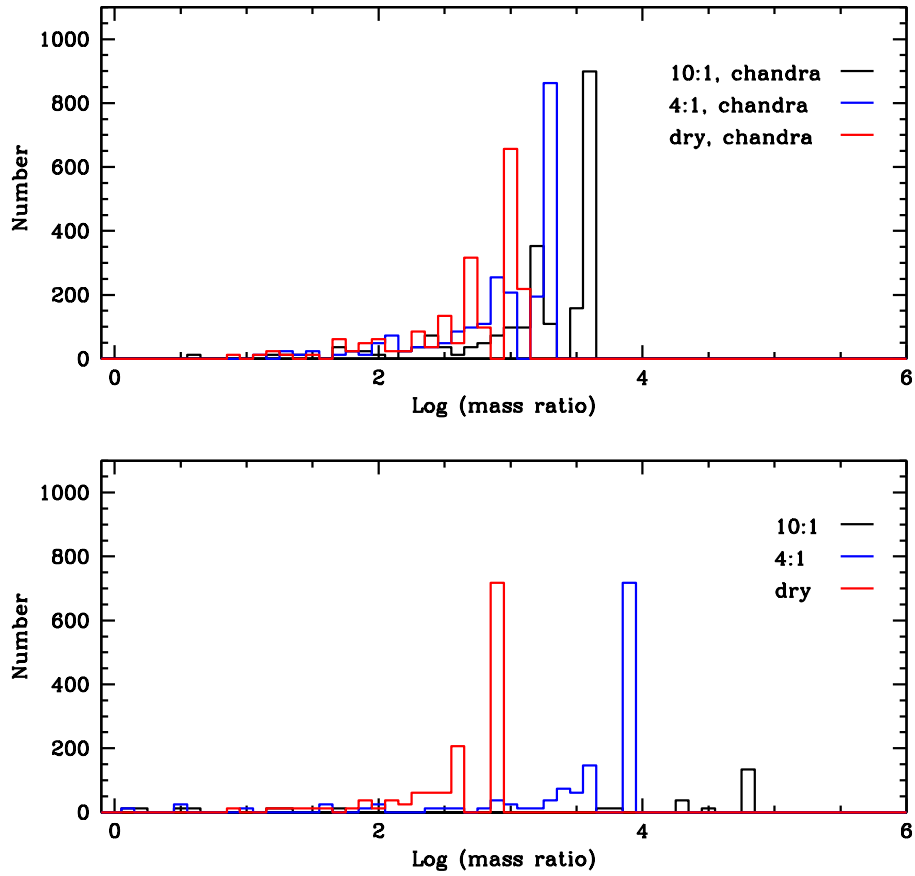


FIG. 4.— Histogram of the mass ratios of sources predicted with a signal-to-noise ratio larger than 5, assuming a 3 year LISA observation. The top panel assumes that the dynamical friction timescale is set by the Chandrasekhar dynamical friction formula, while the bottom panel assumes the Boylan-Kolchin formula. The colors correspond to different black hole growth assumptions: red assumes black holes grow only through mergers, black assumes that gas accretion onto both black holes is triggered if the host dark matter halos have a mass ratio smaller than 10:1, and the blue assumes this accretion only occurs for halo mergers with 4:1 mass ratios. For more detail on the particular black hole growth prescription, see Micic, Holley-Bockelmann, and Sigurdsson 2008. Regardless of the growth prescription or the large-scale dynamics, we see here that LISA observations will be dominated in number by high mass ratio black hole mergers, at least for the assembly of these relatively light supermassive black holes.

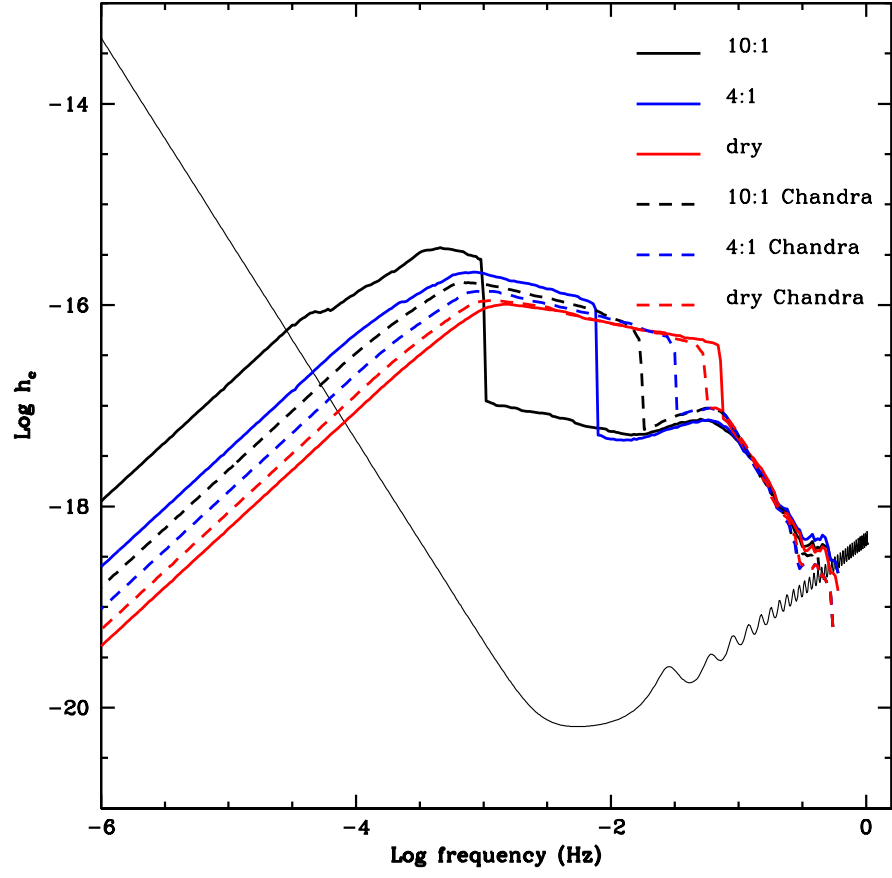


FIG. 5.— Total characteristic strain as a function of observed frequency for all the massive black hole mergers in the cosmological volume for a three year observation. The solid curve is the sensitivity curve for LISA for a single-arm Michaelson configuration.

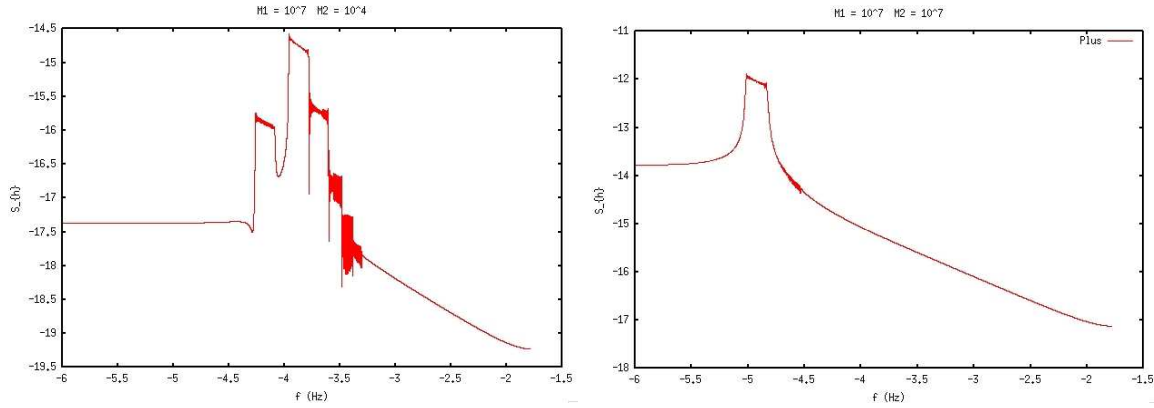


FIG. 6.— The plus polarization of the gravitational wave amplitude as a function of frequency for two representative black hole mergers at redshift 3. Sources are placed at the same random sky position and orientation. Left: merger with black hole masses $M_1 = 10^7 M_\odot$ and $M_2 = 10^4 M_\odot$. Right: merger with equal black hole masses of $10^7 M_\odot$. Notice the broader bandwidth and richer structure of the high mass ratio merger.

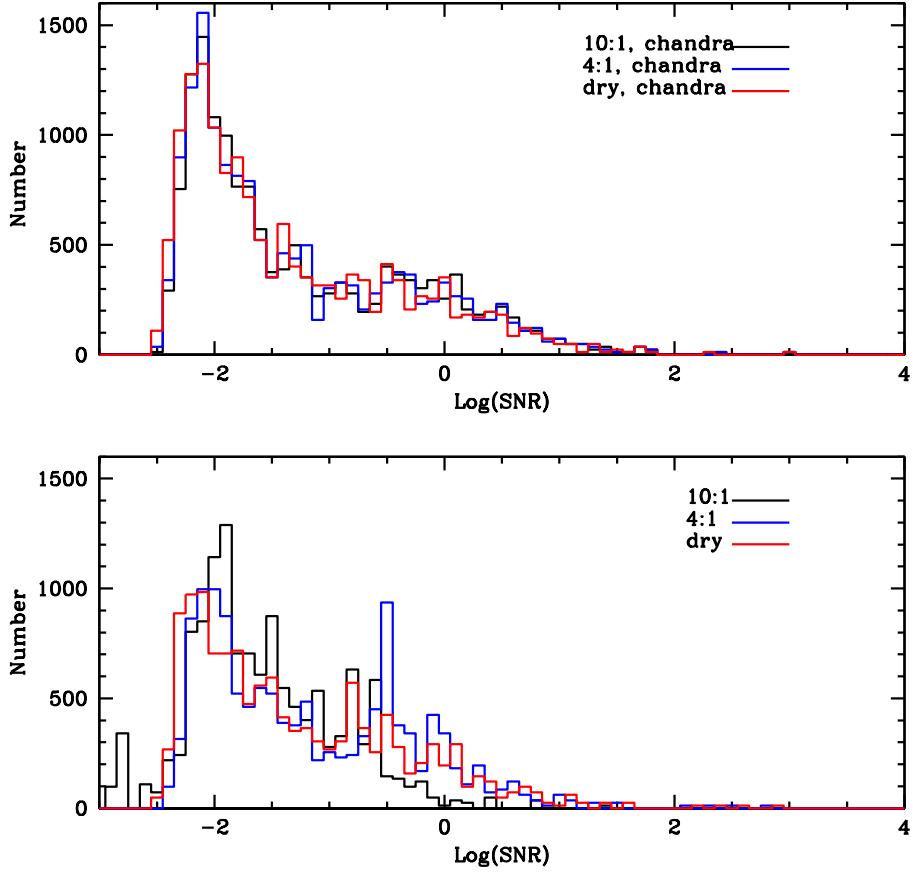


FIG. 7.— Histogram of the signal-to-noise ratio of the black hole mergers in our volume (scaled to cosmological volumes) for an assumed 3-year LISA observation window. See figure 4 for a description of the panels and colors. Since our cosmological volume is small, we are unable to resolve the growth of the most massive black holes. Most of our mergers are at high redshift between seed and intermediate mass black holes involved in assembling the light end of the supermassive black hole spectrum; these high redshift, low mass mergers yield low signal-to-noise sources.

TABLE 1
MAXIMUM REDSHIFT TO OBSERVE MERGERS AT A SIGNAL TO NOISE RATIO OF 5 IN A THREE YEAR LISA OBSERVATION.

M_{bh1}	M_{bh2}	redshift in volume	max redshift
19398	16654	8.881	9.1
83201	20548	7.958	17.5
2723	929	0.726	0.8
46124	9093	1.169	9.8
13054368	435	0.017	0.5
13055368	200	0.006	0.4
13055168	600	0.006	0.5

Column 1: Primary black hole mass. Column 2: Secondary black hole mass. Column 3: Redshift the merger occurred within the simulation volume. Column 4: The redshift to which the merger can be detected at a signal to noise ratio of 5 for a three year LISA observation.

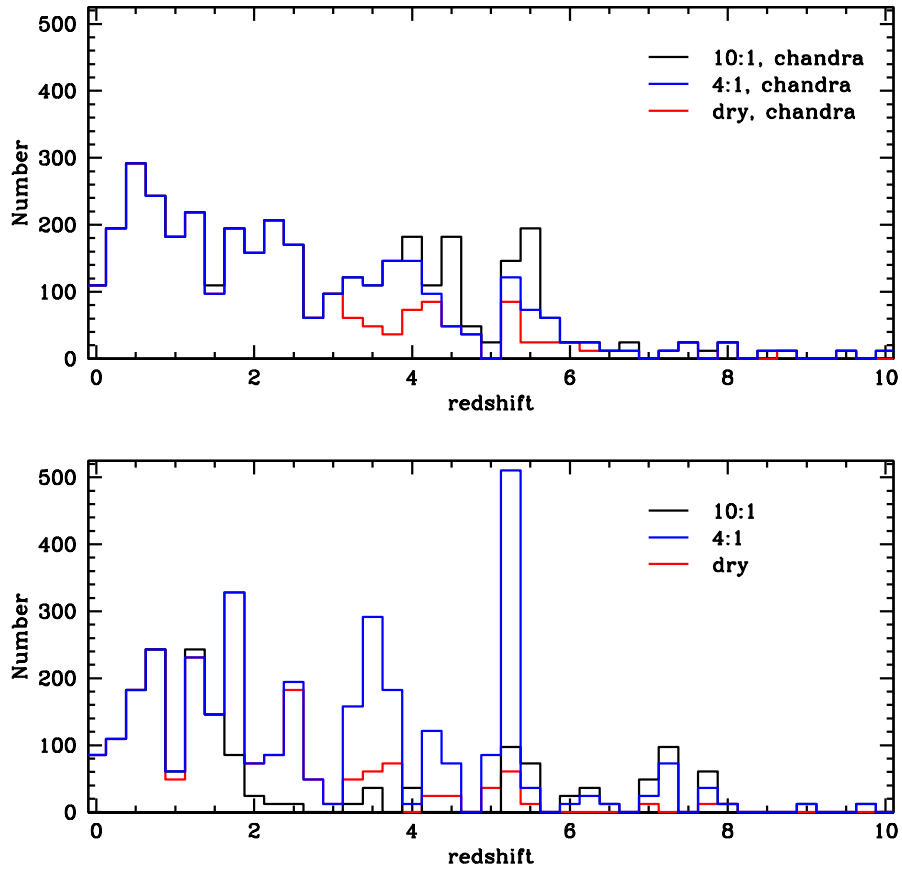


FIG. 8.— Histogram of the redshift of the resolved black hole mergers in our volume (scaled to cosmological volumes) for an assumed 3-year LISA observation window. See figure 4 for a description of the panels and colors. We assume that a signal-to-noise ratio greater than 5 will be resolvable; given the higher mass ratios of a typical merger, however, signal-to-noise ratios higher than 30 may be needed to resolve a source.

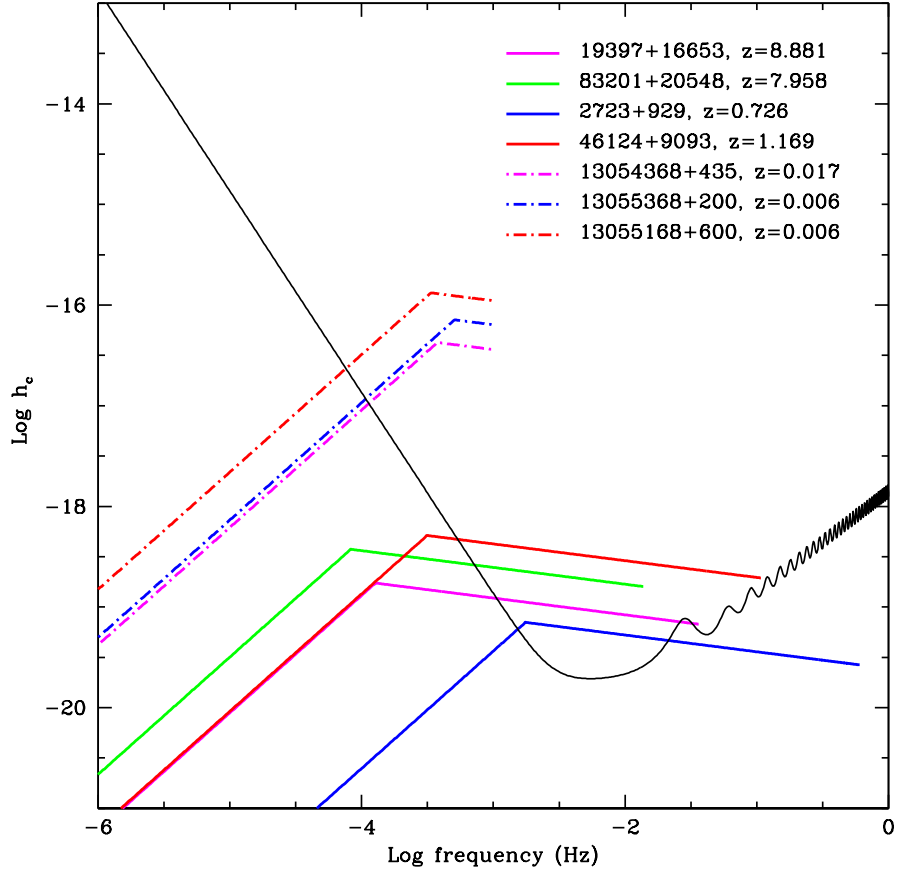


FIG. 9.— Characteristic strain over a 3-year observation for selected classes of resolvable black hole mergers in the simulation as a function of observed frequency. Here, the dynamical friction is treated with a Boylan-Kolchin formula and gas accretion is triggered for dark matter halo mergers with mass ratios smaller than 10:1. The merger redshift and pre-merger masses of the black hole binary are labeled; our loudest sources are either caused by mergers between two intermediate mass black holes, or between a very light seed black hole and the most massive supermassive black hole in our volume.

TABLE 2
NUMBER OF RESOLVABLE BLACK HOLE MERGERS FOR SEVERAL BLACK HOLE GROWTH SCENARIOS.

Gas Accretion Trigger	Dynamical Friction Type	SNR	Observation Time	Number of Mergers
Salpeter 10:1	Chandra	30	10	1033
Salpeter 4:1	Chandra	30	10	741
Dry Mergers	Chandra	30	10	608
Salpeter 10:1	Boylan-Kolchin	30	10	474
Salpeter 4:1	Boylan-Kolchin	30	10	851
Dry Mergers	Boylan-Kolchin	30	10	425
Salpeter 10:1	Chandra	5	10	3768
Salpeter 4:1	Chandra	5	10	3367
Dry Mergers	Chandra	5	10	2892
Salpeter 10:1	Boylan-Kolchin	5	10	1775
Salpeter 4:1	Boylan-Kolchin	5	10	3476
Dry Mergers	Boylan-Kolchin	5	10	2516
Salpeter 10:1	Chandra	30	5	644
Salpeter 4:1	Chandra	30	5	511
Dry Mergers	Chandra	30	5	400
Salpeter 10:1	Boylan-Kolchin	30	5	172
Salpeter 4:1	Boylan-Kolchin	30	5	510
Dry Mergers	Boylan-Kolchin	30	5	280
Salpeter 10:1	Chandra	5	5	2893
Salpeter 4:1	Chandra	5	5	2674
Dry Mergers	Chandra	5	5	2261
Salpeter 10:1	Boylan-Kolchin	5	5	729
Salpeter 4:1	Boylan-Kolchin	5	5	2176
Dry Mergers	Boylan-Kolchin	5	5	1726
Salpeter 10:1	Chandra	30	3	438
Salpeter 4:1	Chandra	30	3	401
Dry Mergers	Chandra	30	3	316
Salpeter 10:1	Boylan-Kolchin	30	3	73
Salpeter 4:1	Boylan-Kolchin	30	3	316
Dry Mergers	Boylan-Kolchin	30	3	194
Salpeter 10:1	Chandra	5	3	2200
Salpeter 4:1	Chandra	5	3	2323
Dry Mergers	Chandra	5	3	1898
Salpeter 10:1	Boylan-Kolchin	5	3	328
Salpeter 4:1	Boylan-Kolchin	5	3	1288
Dry Mergers	Boylan-Kolchin	5	3	1896

Columns 1 and 2 describe the black hole growth model; column 1 indicates which halo mass ratio would trigger gas accretion onto the primary black hole; column 2 indicates the dynamical friction formalism that dictates the gas accretion timescale. Column 3: Signal to noise ratio for detection. Column 4: Observation duration. Column 5: Predicted number of LISA events. Note that column 5 is not the entire LISA event rate; it is the conjectured rate from the class of sources involved in assembling the lightest SMBHs. Also note that although the predicted event rate varies here by a factor of 50, even the most pessimistic rate estimate still will provide ample new sources for LISA to observe.